Synthesis and structural characterization of three zinc coordination complexes based on 3,5-dimethylpyrazole and carboxylate ligands

Shouwen Jin [a] & Daqi Wang [b]

[a] Faculty of Science , ZheJiang A & F University , Lin'An 311300 , P.R. China

[b] Department of Chemistry , Liaocheng University , Liaocheng 252059 , P.R. China
Published online: 25 May 2011.

PLEASE SCROLL DOWN FOR ARTICLE

Taylor & Francis
Taylor & Francis Group

Synthesis and structural characterization of three zinc coordination complexes based on 3,5-dimethylpyrazole and carboxylate ligands

SHOUWEN JIN*† and DAQI WANG‡

†Faculty of Science, ZheJiang A & F University, Lin'An 311300, P.R. China
‡Department of Chemistry, Liaocheng University, Liaocheng 252059, P.R. China

Three new zinc(II) complexes, $Zn(Hdmpz)_2(L1)_2$ (**1**) (Hdmpz = 3,5-dimethylpyrazole, HL1 = 1-hydroxy-2-naphthoic acid), $Zn_2(Hdmpz)_4(L2)_2$ (**2**) (HL2 = maleic acid), and $Zn_3(\mu\text{-dmpz})_4(Hdmpz)_2(L3)$ (**3**) (HL3 = phthalic acid), were prepared and structurally characterized by elemental analysis, infrared spectra, thermogravimetric analysis, and single-crystal X-ray diffraction analysis. X-ray crystallographic studies show that these complexes display mononuclear to coordination polymer structures with a tetrahedral arrangement around each zinc ion. Pyrazole is coordinated both in terminal and bridging in **3**, whereas in **1** and **2** both are coordinated only monodentate. In **1** the carboxylates are monodentate, while in **2** and **3** both function as bridging bis-monodentate ligands. Rich intra- and inter-molecular weak interactions such as classical hydrogen bonds, C–H···O, CH_3···O, C–H···π, and CH_3–π interactions are analyzed.

Keywords: Zinc(II); 3,5-Dimethylpyrazole; Carboxylate ligands; Crystal structure; Non-bonding interaction

1. Introduction

Supramolecular crystal engineering is an area of intense research [1–3] due to fundamental interest in selfassembly processes [4], supramolecular motifs [5], and intriguing structure topologies. The structure depends on coordination geometry of the metal centre, the metal–ligand stoichiometric ratio, the nature of counter ions, weak interactions (hydrogen bonding, aromatic π–π stacking interactions as well as van der Waals forces) [6–8], and various experimental conditions.

Coordination polymers possess functional properties, such as magnetism, catalysis, optical, and sorption properties [9, 10]. A variety of metal ions or more complex metal-containing fragments have been employed, and organic ligands containing O- or N-donors have been widely used [11].

Zn^{2+} is particularly suitable for the construction of coordination polymers, exhibiting a variety of coordination numbers and geometries, tetrahedral, trigonal bipyramidal,

---
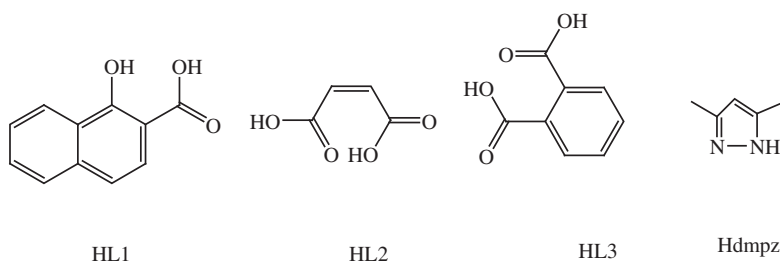
Scheme 1. The ligands used in this article.

square pyramidal, and octahedral, sometimes with a severe distortion. Lability of Zn complexes enables Zn ions and ligands to rearrange during assembly to form highly ordered structures. Consequently, Zn can readily form all kinds of architectures ranging from 1-D to 3-D structures.

Pyrazole and pyrazole derivatives have been widely employed in polypyrazolylborates to stabilize organometallic and coordination compounds [12, 13]. A variety of complexes containing 3,5-dimethylpyrazole (Hdmpz) have been employed in coordination and organometallic chemistry [14–16]. Many complexes with pyrazole as terminal or bridging ligands are also available [17–19]. Complexes with carboxylic acids and pyrazole derivatives are not very common except some recently reported examples [20, 21]. We have been working with coordination compounds with mixed carboxylate and imidazole derivatives [22–24]. Pyrazole and carboxylate appear to possess similar steric requirements and, to a certain extent, also similar bonding capabilities. In order to get a better understanding of the influence of carboxylate in the formation of new coordination polymers and investigate the role that weak non-covalent interactions play in forming the final supramolecular frameworks, we studied the zinc–pyrazolate–carboxylate system. Thus, we report the synthesis, structural characterization, and thermal behavior of three Zn complexes bearing 3,5-dimethylpyrazole (Hdmpz) and different carboxylates (scheme 1), $Zn(Hdmpz)_2(L1)_2$ (**1**) (Hdmpz = 3,5-dimethylpyrazole, L1 = 1-hydroxy-2-naphthoate), $Zn_2(Hdmpz)_4(L2)_2$ (**2**) (L2 = maleate), and $Zn_3(\mu\text{-dmpz})_4(Hdmpz)_2(L3)$ (**3**) (L3 = phthalate).

2. Experimental

2.1. *Materials and physical measurements*

Chemicals and solvents used in this work are of analytical grade, available commercially and were used without purification. FT-IR spectra were recorded as KBr pellets from 4000 to 400 cm^{-1} on a Mattson Alpha-Centauri spectrometer. Microanalytical (C, H, N) data were obtained with a Perkin-Elmer Model 2400II elemental analyzer. Thermogravimetric analyses (TGA) were studied on a Delta Series TA-SDT Q600 under N$_2$ between room temperature and 800°C (heating rate 10°C min^{-1}) using Al crucibles.

2.2. *Synthesis of complexes*

2.2.1. Synthesis of Zn(Hdmpz)$_2$(L1)$_2$ (1). A solution of Zn(CH$_3$COO)$_2 \cdot$ 2H$_2$O (0.0220 g, 0.1 mmol) in 5 mL of MeOH was added to a MeOH solution (8 mL) containing Hdmpz (0.0192 g, 0.2 mmol) and 1-hydroxy-2-naphthoic acid (HL1) (0.0760 g, 0.4 mmol) under continuous stirring. The solution was stirred for 2 h at room temperature until a small amount of precipitate formed; then a few drops of concentrated ammonia were added till the precipitate dissolved completely. The clear red solution was filtered into a test tube and after several days red needle crystals formed, were filtered off, washed with MeOH, and dried under vacuum to afford 0.0800 g of the product. Yield: 63.29% (based on Hdmpz). Elemental analysis performed on crystals exposed to the atmosphere: Calcd for C$_{32}$H$_{30}$N$_4$O$_6$Zn (631.97) (%): C, 60.76; H, 4.75; N, 8.86. Found (%): C, 60.72; H, 4.68; N, 8.79. Infrared (IR) spectrum (KBr disk, cm^{-1}): 3736w, 3444w, 3406w, 3298w, 3132m, 3035m, 2928m, 2865m, 2778 W, 2639 W, 2360 s, 2270 m, 1662 m, 1648 m, 1616 s, 1480 s, 1419 s, 1296 m, 1228 s, 1180 m, 1050 m, 1016 m, 967 m, 882 m, 804 m, 740 m, 688 m, 622 m.

2.2.2. Synthesis of Zn$_2$(Hdmpz)$_4$(L2)$_2$ (2). A solution of Zn(CH$_3$COO)$_2 \cdot$ 2H$_2$O (0.0220 g, 0.1 mmol) in 5 mL of MeOH was added to a MeOH solution (10 mL) containing Hdmpz (0.0192 g, 0.2 mmol) and maleic acid (HL2) (0.0232 g, 0.2 mmol) under continuous stirring. The solution was stirred for 2 h at room temperature and became turbid; then a few drops of conc. ammonia were added till the solution became clear. The clear solution was filtered into a test tube and after several days colorless block crystals formed, were filtered off, washed with MeOH, and dried under vacuum to afford 0.0520 g of the product. Yield: 34.97% (based on Hdmpz). Elemental analysis performed on crystals exposed to the atmosphere: Calcd for C$_{28}$H$_{36}$N$_8$O$_8$Zn$_2$ (743.39) (%): C, 45.20; H, 4.84; N, 15.06. Found (%): C, 45.15; H, 4.76; N, 15.02. IR spectrum (KBr disk, cm^{-1}): 3568 m, 3428 m, 3236w, 3142w, 3072w, 2974 m, 2858 m, 2540 s, 2520 m, 2320 m, 1622 s, 1598 s, 1550 m, 1520 s, 1448 m, 1424 s, 1292 m, 1227 m, 1198 m, 1056 m, 1014 m, 940 m, 902 m, 828 m, 768(m), 692 m, 646 m, 612 m.

2.2.3. Synthesis of Zn$_3$(μ-dmpz)$_4$(Hdmpz)$_2$(L3) (3). A solution of Zn(CH$_3$COO)$_2 \cdot$ 2H$_2$O (0.0220 g, 0.1 mmol) in 5 mL of EtOH was added to an EtOH solution (8 mL) containing Hdmpz (0.0192 g, 0.2 mmol) and phthalic acid (HL3) (0.0322 g, 0.2 mmol) under continuous stirring. The solution was stirred for 2 h at room temperature and became turbid. A few drops of conc. ammonia were added till the solution became clear. The clear solution was filtered into the test tube, after several days colorless crystals formed, were filtered off, washed with EtOH, and dried under vacuum to afford 0.0620 g of the product. Yield: 33.22% (based on Hdmpz). Elemental analysis performed on crystals exposed to the atmosphere: Calcd for C$_{38}$H$_{48}$N$_{12}$O$_4$Zn$_3$ (932.99): C, 48.88; H, 5.14; N, 18.01. Found (%): C, 48.82; H, 5.04; N, 17.89. IR spectrum (KBr disk, cm^{-1}): 3442 s, 3321 s, 3140 m, 3060 m, 2990 m, 2949w, 2812 m, 2720 m, 2540w, 2360 m, 2190 m, 1960w, 1840w, 1800w, 1775w, 1730 m, 1670 s, 1596 s, 1520 s, 1460 s, 1402 s, 1289 m, 1245 m, 1153 m, 1102 m, 1064 m, 952 m, 886 m, 832 m, 780 m, 740 m, 680 m, 660 m, 657 m, 620 m.

2.3. *X-ray crystallography*

Suitable crystals were mounted on a glass fiber on a Bruker SMART 1000 CCD diffractometer operating at 50 kV and 40 mA using Mo-Kα radiation (0.71073 Å). Data collection and reduction were performed using *SMART* and *SAINT* software [25]. The structures were solved by direct methods and non-hydrogen atoms were subjected to anisotropic refinement by full-matrix least-squares on F^2 using *SHELXTL* [26]. Hydrogen positions for all of the structures were found in a difference map. Further details of the structural analysis are summarized in table 1. Selected bond lengths and angles for **1**, **2**, and **3** are listed in table 2 and relevant hydrogen bond parameters are provided in table 3.

3. Results and discussion

3.1. *Preparation and characterization*

Complexes **1–3** were prepared in MeOH or EtOH at room temperature *via* combination of *zinc* acetate, Hdmpz group, and the corresponding carboxylic acid. Crystals suitable for X-ray crystallographic analysis were grown upon addition of a few drops of conc. ammonia solution with yields of 33.22–63.29%.

During the process acetate is substituted by the corresponding carboxylate, and some Hdmpzs retain NH groups, and some are deprotonated. These compounds are not soluble in most common solvents. The IR spectra of **1–3** were fully consistent with their formulations. IR spectra of **1**, **2**, and **3** display characteristic carboxylate bands at 1560–1622 cm^{-1} for $\nu_{as}(CO_2)$ and at 1400–1430 cm^{-1} for $\nu_s(CO_2)$ [27]. The frequency differences between $\nu_{as}(CO_2)$ and $\nu_s(CO_2)$ are 197, 174, and 194 cm^{-1} for **1**, **2**, and **3**, respectively, suggesting unidentate coordination for carboxylate. Neutral coordinated Hmdpz in all three compounds is confirmed by the presence of characteristic NH bands at 3400–3000 cm^{-1} [28]. Weak absorptions observed at 2800–2600 cm^{-1} can be attributed to aromatic C–H and CH of L2.

3.2. *Crystal structure descriptions*

3.2.1. Crystal and molecular structure of Zn(Hdmpz)₂(L1)₂ (1).
Compound **1** prepared by the reaction of $Zn(CH_3COO)_2 \cdot 2H_2O$, 1-hydroxy-2-naphthoic acid (HL1), and Hdmpz in MeOH with ratios of 1 : 2 : 4 yields pure Zn(Hdmpz)₂(L1)₂ upon addition of a few drops of concentrated ammonia solution. The structure determination reveals that Zn, L1, and Hdmpz are present in a 1 : 2 : 2 ratio; the asymmetric unit is shown in figure 1. Complex **1** crystallizes in triclinic system with space group $P\bar{1}$.

Each zinc is tetrahedrally coordinated by two oxygens of two monodentate L1 and by two nitrogens, belonging to two monodentate pyrazoles (figure 1). The molecular structure of **1** resembles $[Zn(CH_3COO)_2(ML)_2]$ monomers, in which ML is a monodentate nitrogen ligand, such as imidazole [29] and pyridine [30].

The location of the H2 and H4 in **1**, bound to nitrogen, and not to oxygen, is consistent with the different acidic characters of pyrazole and 1-hydroxy-2-naphthoic acid [20], and also confirmed by the difference electron density map which found

Table 1. Summary of X-ray crystallographic data for **1**, **2**, and **3**.

	1	2	3
Empirical formula	$C_{32}H_{30}N_4O_6Zn$	$C_{28}H_{36}N_8O_8Zn_2$	$C_{38}H_{48}N_{12}O_4Zn_3$
Formula weight	631.97	743.39	932.99
Temperature (K)	298(2)	298(2)	298(2)
Wavelength (Å)	0.71073	0.71073	0.71073
Crystal system	Triclinic	Monoclinic	Monoclinic
Space group	$P\bar{1}$	$P2(1)/c$	$C2$
Unit cell dimensions (Å, °)			
a	8.8600(10)	9.4027(7)	16.7428(15)
b	10.6081(13)	15.8078(16)	13.9259(12)
c	16.8129(18)	22.124(2)	11.5382(11)
α	86.053(2)	90	90
β	77.8250(10)	96.7110(10)	127.671(2)
γ	74.1440(10)	90	90
Volume (Å³), Z	1485.8(3), 2	3265.8(5), 4	2129.4(3), 2
Calculated density ($Mg\,m^{-3}$)	1.413	1.512	1.455
Absorption coefficient (mm^{-1})	0.878	1.529	1.729
$F(000)$	656	1536	964
Crystal size (mm^3)	$0.45 \times 0.38 \times 0.26$	$0.32 \times 0.26 \times 0.24$	$0.25 \times 0.23 \times 0.21$
θ range for data collection (°)	2.34–25.02	1.59–25.02	2.12–25.01
Limiting indices	$-9 \leq h \leq 10; -12 \leq k \leq 12; -20 \leq l \leq 17$	$-5 \leq h \leq 11; -17 \leq k \leq 18; -26 \leq l \leq 24$	$-19 \leq h \leq 11; -16 \leq k \leq 15; -11 \leq l \leq 13$
Reflections collected	7733	16052	5421
Independent reflections	5165 [R(int) = 0.0208]	5748 [R(int) = 0.1048]	3597 [R(int) = 0.0688]
Goodness-of-fit on F^2	1.013	1.024	0.995
R indices [$I > 2\sigma(I)$]	0.0405, 0.0861	0.0641, 0.1508	0.0620, 0.1533
R indices (all data)	0.0693, 0.1007	0.1265, 0.1932	0.0728, 0.1613
Largest difference peak and hole (e Å^{-3})	0.368 and −0.248	1.334 and −0.509	0.854 and −0.762

Table 2. Selected bond lengths [Å] and angles [°] for **1**, **2**, and **3**.

1

Zn(1)–O(1)	1.935(2)	Zn(1)–O(4)	1.948(2)
Zn(1)–N(1)	1.993(2)	Zn(1)–N(3)	2.002(2)
O(1)–C(11)	1.263(4)	O(2)–C(11)	1.269(4)
O(3)–C(12)	1.348(4)	O(4)–C(22)	1.266(4)
O(5)–C(22)	1.263(4)	O(6)–C(23)	1.340(3)
O(1)–Zn(1)–O(4)	102.68(10)	O(1)–Zn(1)–N(1)	116.00(10)
O(4)–Zn(1)–N(1)	106.97(9)	O(1)–Zn(1)–N(3)	102.40(10)
O(4)–Zn(1)–N(3)	110.71(10)	N(1)–Zn(1)–N(3)	117.17(10)
O(1)–C(11)–O(2)	123.3(3)	O(5)–C(22)–O(4)	124.0(3)

2

Zn(1)–O(5)	1.893(5)	Zn(1)–O(1)	1.937(5)
Zn(1)–N(3)	1.988(6)	Zn(1)–N(1)	2.006(6)
Zn(2)–O(3)	1.907(5)	Zn(2)–O(7)	1.936(5)
Zn(2)–N(5)	1.986(6)	Zn(2)–N(7)	2.015(6)
O(1)–C(1)	1.239(8)	O(2)–C(1)	1.220(8)
O(3)–C(4)	1.259(8)	O(4)–C(4)	1.203(8)
O(5)–C(5)	1.263(8)	O(6)–C(5)	1.206(8)
O(7)–C(8)	1.243(8)	O(8)–C(8)	1.210(8)
O(5)–Zn(1)–O(1)	110.8(2)	O(5)–Zn(1)–N(3)	118.3(2)
O(1)–Zn(1)–N(3)	115.2(2)	O(5)–Zn(1)–N(1)	101.8(2)
O(1)–Zn(1)–N(1)	102.1(2)	N(3)–Zn(1)–N(1)	106.3(2)
O(3)–Zn(2)–O(7)	105.7(2)	O(3)–Zn(2)–N(5)	120.8(2)
O(7)–Zn(2)–N(5)	115.2(2)	O(3)–Zn(2)–N(7)	104.3(2)
O(7)–Zn(2)–N(7)	106.9(2)	N(5)–Zn(2)–N(7)	102.5(2)

3

Zn(1)–O(1)	1.960(6)	Zn(1)–N(1)	1.979(6)
Zn(1)–N(3)	1.980(6)	Zn(1)–N(5)	2.026(7)
Zn(2)–N(2)	1.999(6)	Zn(2)–N(4)	2.001(7)
O(1)–C(16)	1.241(11)	O(2)–C(16)	1.27(4)
O(2')–C(16)	1.24(5)	O(1)–Zn(1)–N(1)	124.5(3)
O(1)–Zn(1)–N(3)	102.5(3)	N(1)–Zn(1)–N(3)	110.0(2)
O(1)–Zn(1)–N(5)	101.3(3)	N(1)–Zn(1)–N(5)	108.2(3)
N(3)–Zn(1)–N(5)	109.5(3)	N(2)#1–Zn(2)–N(2)	109.3(4)
N(2)#1–Zn(2)–N(4)	106.4(3)	N(2)–Zn(2)–N(4)	109.5(2)
N(4)–Zn(2)–N(4)#1	115.6(4)		

Symmetry transformations used to generate equivalent atoms for **3**: #1 $-x+1, y, -z+1$.

Table 3. Hydrogen bond distances and angles in **1**, **2**, and **3**.

D–H···A	d(D–H) [Å]	d(H···A) [Å]	d(D···A) [Å]	∠(DHA) [°]
1				
O(6)–H(6)···O(5)	0.82	1.82	2.551(3)	147.4
N(4)–H(4)···O(5)	0.86	1.97	2.724(3)	144.9
N(2)–H(2)···O(2)	0.86	1.93	2.718(3)	151.0
2				
N(8)–H(8)···O(6)#2	0.86	1.97	2.795(8)	161.4
N(6)–H(6)···O(8)	0.86	1.91	2.669(8)	146.9
N(4)–H(4)···O(2)	0.86	1.85	2.640(8)	152.2
N(2)–H(2)···O(4)	0.86	1.86	2.701(7)	167.5
3				
N(6)–H(6)···O(2')#2	0.86	1.99	2.72(3)	141.4
N(6)–H(6)···O(2)#2	0.86	1.97	2.74(3)	148.1

Symmetry transformations used to generate equivalent atoms for **2**: #2 $x+1, -y+1/2, z+1/2$; for **3**: #2 $-x+2, y, -z+2$.
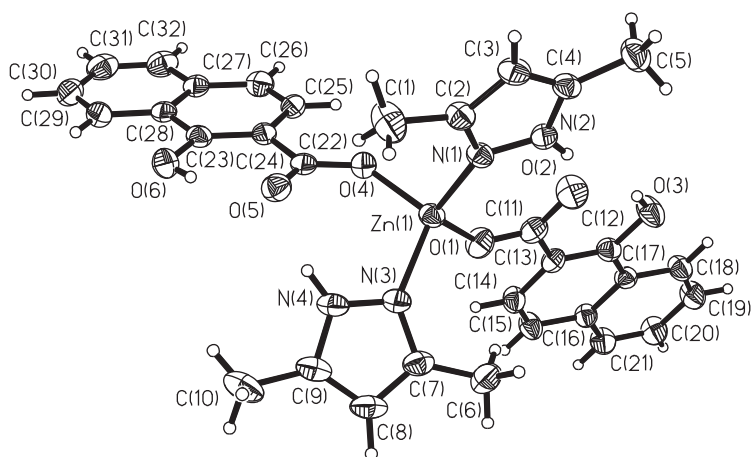
Figure 1.   Molecular structure of **1** showing the atom numbering scheme at 30% ellipsoid probability level.

the hydrogens. ZnN_2O_2 possesses coordination distances and angles in the ranges of 1.935(2)–2.002(2) Å and 102.40(10)–117.17(10)°, respectively; the overall coordination geometry resembles that found in $[Zn(Hpz)_2(Me_3NCH_2CO_2)](ClO_4)_2$ [21] and $\{[Zn(CH_3COO)_2(Hpz)_2]\cdot CH_3COOH\}$ (Hpz = pyrazole) [20a]. Although the distortion in the ZnN_2O_2 moiety is differently oriented in the latter two compounds, the angles around zinc are 98.94(19)–117.30(18)° and 95.73(7)–118.34(8)°, respectively. Compound **1** is not an ionic species consisting of monocationic zinc(II) complex and carboxylate counterions. In **1**, the non-bonded oxygens, far enough from zinc with distances of 3.245 and 3.287 Å, respectively, are involved in two intramolecular hydrogen bonds (N(2)–H(2)···O(2) and N(4)–H(4)···O(5)) with the N–O distances ranging from 2.718(3) to 2.724(3) Å and H–O distances of 1.93–1.97 Å. In addition to the intramolecular N–H···O hydrogen bonds, there also exist intramolecular O–H···O hydrogen bonds (table 3) between phenol OH and the non-bonded oxygen of L1 to produce a $S_1^1(6)$ loop motif according to Bernstein *et al.* [31], thus the non-bonded oxygen forms two hydrogen bonds in bifurcate mode.

The root mean square (rms) deviations of the pyrazole rings containing N1 and N2; and N3 and N4 are 0.0113 and 0.0038 Å, respectively, making a dihedral angle of 52°. The rms deviation of the naphthalene ring containing C(12)–C(21) is 0.0067 Å, which forms dihedral angles of 4.2° and 56° with the above two pyrazole rings, respectively, indicating the co-planarity of the naphthalene ring bearing C(12)–C(21) and one pyrazole. The rms deviation of the naphthalene ring bearing C(23)–C(32) is 0.0055 Å, which forms a dihedral angle of 68.8° with the naphthalene ring containing C(12)–C(21). The interplane angles between the naphthalene ring containing C(23)–C(32) and the two pyrazole rings bearing N1 and N2; and N3 and N4 are 72.9° and 124.7°, respectively.

The mononuclear units are connected through C–H···π interaction (with the C–Cg distance of *ca* 3.408 Å) between 4-CH of the pyrazole and the pyrazole of the neighboring mononuclear unit to form a 1-D chain running along the *a*-axis. The Zn···Zn distance along the chain is 8.860 Å, while the Zn···Zn distance between two adjacent chains is 8.339 Å. Adjacent chains were further connected through CH_3···O
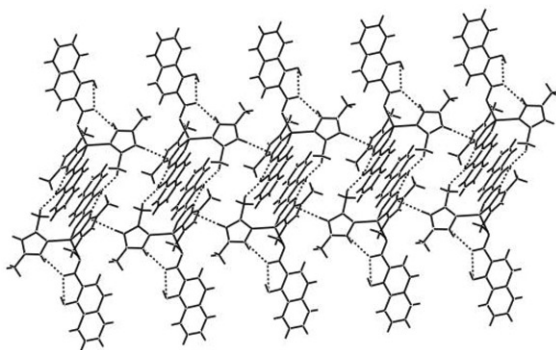
Figure 2. Packing diagram of **1** showing the 1-D double chain structure viewed along the *b*-axis.
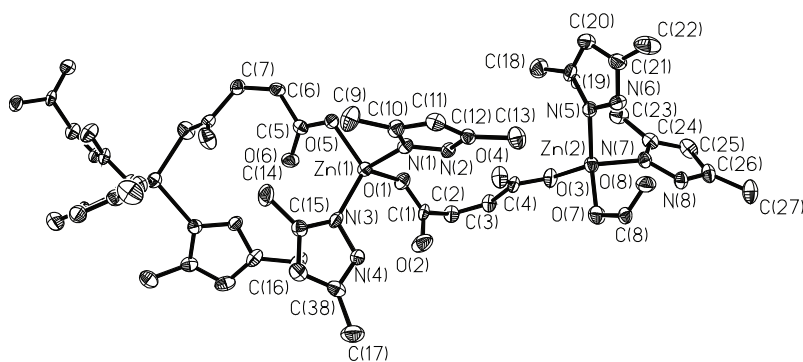
Figure 3. Molecular structure of **2** showing the atom numbering scheme at 30% ellipsoid probability level.

(between the 3-CH$_3$ of pyrazole and phenol OH with C–O distance of 3.409 Å) interactions to form a 2-D double-chain structure, which is shown in figure 2. The corresponding ligands on these two chains are antiparallel.

3.2.2. Crystal and molecular structure of Zn$_2$(Hdmpz)$_4$(L2)$_2$ (2). Crystals of **2** contain dinuclear [Zn$_2$(Hdmpz)$_4$(L2)$_2$] (figure 3). Compound **2** crystallizes as monoclinic colorless blocks in the space group *P*2(1)/*c*, and there are four formula units in its cell. Each zinc is tetrahedrally coordinated by two oxygens of two monodentate L2 and by two nitrogens, belonging to two monodentate pyrazoles with ZnN$_2$O$_2$. The ZnN$_2$O$_2$ unit possesses coordination distances and angles in the ranges 1.893(5)–2.015(6) Å and 102.1(2)–120.8(2)°, respectively. The geometrical parameters of this species are similar to **1**; in **2** the Zn has the same coordination mode as that of **1** except that the dicarboxylate L2 substitute the monocarboxylate L1 ligands present in **1**.

The C(2)=C(3) and C(6)=C(7) bond distances (1.300(9) and 1.290(9) Å) are for a simple C=C double bond, due to the significant non-coplanarity of the carboxyl and the olefinic groups. The C–O bond distances involving oxygen coordinated to Zn are
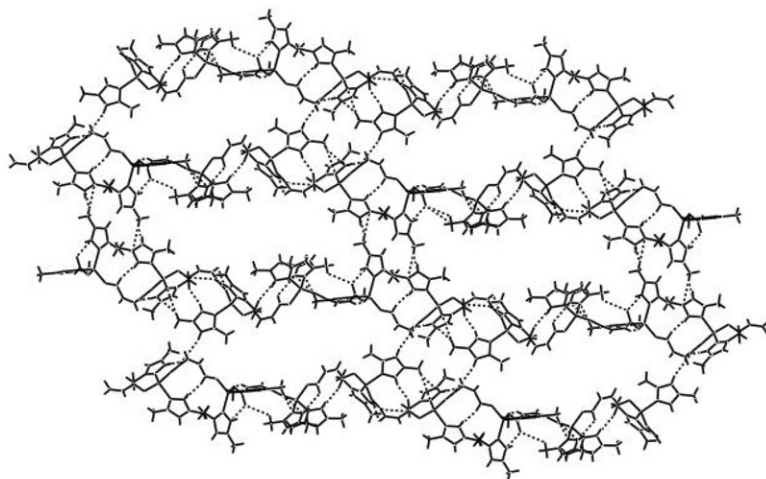
Figure 4. Packing diagram of **2** showing the 2-D sheet structure viewed down the *a*-axis.

longer than C–O distances that did not coordinate with zinc although they form some non-bonding interactions.

The rms deviations of the two pyrazole rings coordinated to Zn1 are 0.0044 and 0.0146 Å, respectively. The rms deviations of the two pyrazole rings coordinated to Zn2 are 0.0039 and 0.0122 Å, respectively. The pair of pyrazoles coordinated to the same Zn have dihedral angles of 83.4° for Zn1 and 87.4° for Zn2, indicating an almost perpendicular arrangement of the rings. The dihedral angles between pyrazole rings coordinated to different Zn cations are 121.8°, 92.6°, 123.4°, and 38°.

The zinc ions do not have any bonding interaction with the "second" oxygen of each dicarboxylate, which is found at a distance of 2.898–3.117 Å from Zn. In **2**, the non-bonded oxygens form four intramolecular N–H···O hydrogen bonds with N–O and H···O distances of 2.640(8)–2.795(8) and 1.85–1.97 Å, respectively.

The maleates adopt one coordination mode in **2**: two carboxyl groups of a maleic acid ligand are both deprotonated and coordinated to adjacent Zn(II) ions in bridging bis-monodentate mode. Thus, the neighboring Zn's are bridged sequentially by carboxylate of maleate forming 1-D infinite helical chained framework running along the *c*-axis. In the chain adjacent Zn–Zn separations are 7.165 and 7.203 Å. In the chain there are some weak non-bonding interactions such as CH_3–π (between the 5-CH_3 of one pyrazole and its adjacent pyrazole ring with C–Cg distance of 3.582 Å) and CH_3–O interactions (between 3-CH_3 of the pyrazole and the non-bonded oxygen of L2 with C–O distance of 3.190 Å). There are also CH–O interactions between CH of the olefinic group of L2 and the non-bonded oxygen of the same L2 with C–O distance of 2.310 Å.

Adjacent chains are connected by the interchain CH–O interaction between 4-CH of the pyrazole and the non-bonded oxygen of the maleate to form a double chain extending along the *c*-axis. Such double chains were further joined together by CH_3–π interaction between 5-CH_3 of the pyrazole at one chain and the pyrazole ring of its neighboring chain with C–Cg distance of *ca* 3.591 Å to form a sheet extending on the *bc* plane as shown in figure 4. In the sheet there are cavities formed by two adjacent chains
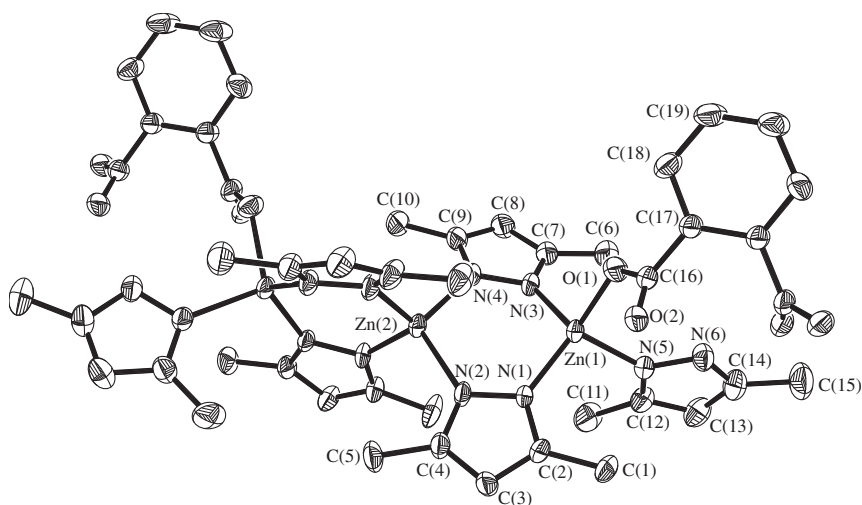
Figure 5.   Molecular structure of **3** showing the atom numbering scheme at 30% ellipsoid probability level.

through weak interactions. The sheets are stacked along the *a*-axis through two kinds of CH–O interactions, one is between the 4-CH of the pyrazole and the non-bonded oxygen of the maleate with C–O distance of 3.300 Å and the other is between the olefinic CH of the maleate and the non-bonded oxygen with C–O distance of 3.356 Å. In this case the second sheet slipped some distance from the first sheet, and the third sheet layer has the same projection on the *bc* plane as the first sheet. The stacking of **2** displays a 3-D layer network structure without channels.

3.2.3. Crystal and molecular structure of Zn$_3$(μ-dmpz)$_4$(Hdmpz)$_2$(L3) (3).   Trinuclear **3** crystallizes in the monoclinic system with space group *C*2. An asymmetric unit of Zn$_3$(μ-dmpz)$_4$(Hdmpz)$_2$(L3) contains 1.5 four-coordinated Zn(II) ions, a half of L3 anion, one Hdmpz, and two dmpz anions (figure 5). The difference between **3**, and **1** and **2** lies in the fact that in **1** and **2** there do not exist bridging pyrazolates; **1** and **2** only have neutral nitrogen ligands.

In the trinuclear units of **3** the two terminal Zn ions are tetrahedral with one oxygen of a monodentate L3 and three nitrogens from one monodentate pyrazole and to two different bridging pyrazolates with ZnN$_3$O binding. The middle Zn is coordinated by four bridging pyrazolates with ZnN$_4$ binding. The pyrazolates are *N,N′*-exobidentate, keeping zinc ions at a non-bonding distance of 3.580 Å, somewhat shorter than the Zn···Zn separation of 3.62 Å in [{Zn(μ-C$_2$H$_5$COO)(μ-pz*)(Hpz*)}$_2$] [32] (Hpz* = 4-acetyl-3-amino-5-methylpyrazole) and [{Zn(μ-C$_2$H$_5$COO)(μ-pz)(Hpz)}$_2$] [21] (Hpz = pyrazole) comsplexes. Similar to **2**, L3 also is bridging bis-monodentate coordination. The ZnN$_3$O unit possesses coordination distances and angles of 1.960(6)–2.026(7) Å and 101.3(3)–124.5(3)°, respectively. The ZnN$_4$ unit possesses coordination distances and angles 1.999(6)–2.001(7) Å and 106.4(3)–115.6(4)°, respectively.

The zinc ions do not have any bonding interaction with the non-coordinated oxygen of carboxylate, which is 3.262 Å from Zn, shorter than the reported average distance of
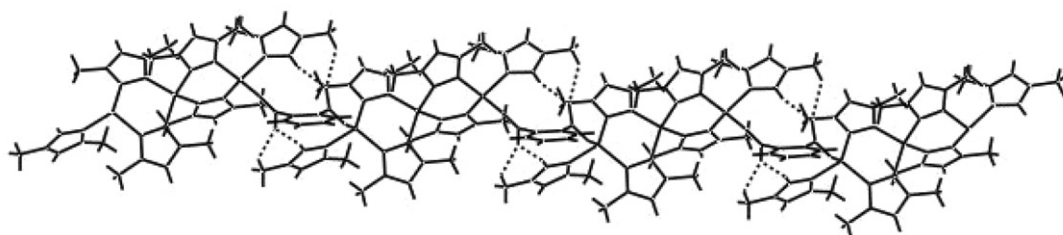
Figure 6. 1-D chain structure of **3** viewed from the *c*-axis.

Table 4. TGA data for **1–3**.

| Stage | Temperature range (°C) | Weight loss (%) | | Probable composition of removed molecules | Complexes |
		Obsd.	Calcd.		
I	164.6–262.8	30.27	30.38	Two pyrazole molecules	**1**
II	285.0–402.0	58.86	58.92	Two L1 ligands	
I	171.0–285.0	51.56	51.65	Four pyrazole molecules	**2**
II	298.0–418.0	30.61	30.69	Two L2 ligands	
I	158.4–249.8	20.47	20.58	Two terminal pyrazole molecules	**3**
II	285.4–418.6	17.54	17.58	One L3 ligand	
III	430.7–613.9	40.62	40.73	Two bridging pyrazolates	

3.398 Å by Singh *et al.* [20c]. In **3**, the non-bonded oxygens form an intramolecular hydrogen bond (N(6)–H(6)···O(2)#2) with N(6)–O(2) and H(6)–O(2) of distances 2.74(3) and 1.97 Å, respectively.

The rms deviations of the pyrazole rings containing N5 and N6; and N1 and N2 are 0.0122 and 0.0130 Å, respectively; the dihedral angle between the two rings is 79.3°. The rms deviation of the pyrazolate ring containing N3 and N4 is 0.0201 Å, forming dihedral angles of 103.7° and 27° with the above two pyrazole rings. The carboxylates deviate by 116.6° from the benzene ring plane of the phthalate.

Compound **3** consists of two planar six-membered [Zn(μ-dmpz)$_2$Zn] cores with the two six-membered rings spiro-fused together by the middle Zn. In the trinuclear unit there are two inversion centers located about the center of each six-membered [Zn(μ-dmpz)$_2$Zn] ring (figure 6). The two six-membered [Zn(μ-dmpz)$_2$Zn] rings were not coplanar with torsion angle of *ca* 130°. The trinuclear moieties are connected by the CH$_3$–O interaction between the 5-CH$_3$ of the terminal pyrazole and the non-bonded oxygen of the adjacent trinuclear unit with C–O distance of 3.231 Å, forming a 1-D chain along the *a*-axis as shown in figure 6. The Zn–Zn separation between two adjacent trinuclear moieties is 6.914 Å, which is significantly larger than the Zn–Zn distance in the same trinuclear aggregate.

3.3. *Thermogravimetry*

The thermal decomposition of **1–3** can be divided into two or three stages according to the temperature range listed in table 4. Neutral pyrazoles were first removed between

158.4°C and 285.0°C; the monodentate carboxylates were lost in the second stage from 285.0°C to 418.6°C. For **3**, the bridging pyrazolates decomposed at 430.7–613.9°C.

4. Summary

Three zinc complexes with 3,5-dimethylpyrazole and different carboxylates have been synthesized and characterized by X-ray diffraction analysis, IR, and thermal analysis. Although synthesized by the same method they showed mononuclear to polymer structures. The central metal ions are coordinated in N_2O_2, N_3O, and N_4 fashions. Crystallographic studies demonstrate that the zinc centers are coordinated only by 3,5-dimethylpyrazole or by both 3,5-dimethylpyrazole and its deprotonated anion; every carboxylate is monodentate toward the metal. The strong structural propensity toward tetracoordination seems to disfavor the formation of ''paddlewheel'' dimeric complexes [30, 33]. In the three coordination compounds different Zn–Zn distances are observed for alternate pairs of zinc ions in the corresponding aggregate. For example in **1**, the Zn–Zn distance between alternate pairs in the same chain is 8.860 Å. In **2**, the distances are 7.165 and 7.203 Å, respectively, between adjacent Zn ions of the same chain. In **3**, this distance is 3.580(1) Å. The non-bonded oxygens of carboxylates are involved in the formation of intramolecular hydrogen bonds with N–H of 3,5-dimethylpyrazole. Although **2** and **3** contain the dicarboxylate with almost the same spacer length between carboxylates, the structure of the metal coordination complexes are obviously different, one with dinuclear [$Zn_2(Hdmpz)_4(L2)_2$] and the other with trinuclear [$Zn_3(\mu\text{-}dmpz)_4(Hdmpz)_2(L3)$]. Complexes **1–3** have abundant intra- and inter-molecular weak interactions (including classical hydrogen bonds, C–H$\cdots$O, $CH_3\cdots$O, C–H$\cdots\pi$, and CH_3–π interactions) in their crystals, which stabilize the final 1-D double chain, 3-D layer network, and 1-D chain structures.

Supplementary material

Acknowledgments

References

[1] B.H. Northrop, Y.R. Zheng, K.W. Chi, P.J. Stang. *Acc. Chem. Res.*, **42**, 1554 (2009).

[2] J.P. Zhang, S.L. Zheng, X.C. Huang, X.M. Chen. *Angew. Chem. Int. Ed.*, **43**, 206 (2004).

[3] N.W. Ockwig, O. DelgadoFriedrichs, M. O'Keeffe, O.M. Yaghi. *Acc. Chem. Res.*, **38**, 176 (2005).

[4] S.P. Wu, C.H. Lee. *CrystEngComm.*, **11**, 219 (2009).

[5] V.A. Blatov, L. Carlucci, G. Ciani, D.M. Proserpio. *CrystEngComm.*, **6**, 378 (2004).

[6] B.J. Holliday, C.A. Mirkin. *Angew. Chem. Int. Ed.*, **40**, 2023 (2001).

[7] J.W. Lee, E.A. Kim, Y.J. Kim, Y.A. Lee, Y. Pak, O.S. Jung. *Inorg. Chem.*, **44**, 3151 (2005).

[8] C.Y. Su, A.M. Goforth, M.D. Smith, H.C. zur Loye. *Inorg. Chem.*, **42**, 5685 (2003).

[9] See, for example: (a) A.M. Kutasi, D.R. Turner, P. Jensen, B. Moubaraki, S.R. Batten, K.S. Murray. *CrystEngComm.*, **11**, 2089 (2009); (b) J.A. Hoshiko, G.B. Wang, J.W. Ziller, G.T. Yee, A.F. Heyduk. *Dalton Trans.*, 5712 (2008); (c) J.Y. Zhang, Y. Ma, A.L. Cheng, Q. Yue, Q. Sun, E.Q. Gao. *Dalton Trans.*, 2061 (2008); (d) C. Janiak, J.K. Vieth. *New J. Chem.*, **34**, 2366 (2010); (e) J.P. Zou, G.W. Zhou, X. Zhang, M.S. Wang, Y.B. Lu, W.W. Zhou, Z.J. Zhang, G.C. Guo, J.S. Huang. *CrystEngComm.*, **11**, 972 (2009); (f) O.M. Yaghi, M. O'Keeffe, N.W. Ockwig, H.K. Chae, M. Eddaoudi, J. Kim. *Nature*, **423**, 705 (2003); (g) G. Férey. *Chem. Soc. Rev.*, **37**, 191 (2008); (h) X.Q. Zhao, P. Cui, B. Zhao, W. Shi, P. Cheng. *Dalton Trans.*, 805 (2011).

[10] C. Janiak. *J. Chem. Soc., Dalton Trans.*, 2781 (2001).

[11] A.Y. Robin, K.M. Fromm. *Coord. Chem. Rev.*, **250**, 2127 (2006).

[12] Y.H. Xing, Y.H. Zhang, Z. Sun, L. Ye, Y.T. Xu, M.F. Ge, B.L. Zhang, S.Y. Niu. *J. Biol. Chem.*, **101**, 36 (2007).

[13] L.M.R. Hill, M.K. Taylor, V.W. Lin Ng, C.G. Young. *Inorg. Chem.*, **47**, 1044 (2008).

[14] K. Umakoshi, T. Kojima, K. Saito, S. Akatsu, M. Onishi, S. Ishizaka, N. Kitamura, Y. Nakao, S. Sakaki, Y. Ozawa. *Inorg. Chem.*, **47**, 5033 (2008).

[15] B. Machura, M. Jaworska, R. Kruszynski. *Polyhedron*, **23**, 2523 (2004).

[16] Y.J. Sun, B. Zhao, P. Cheng. *Inorg. Chem. Commun.*, **10**, 583 (2007).

[17] (a) A.A. Mohamed, S. Ricci, A. Burini, R. Galassi, C. Santini, G.M. Chiarella, D.Y. Melgarejo, J.P. Fackler Jr. *Inorg. Chem.*, **50**, 1014 (2011); (b) R. Mukherjee. *Coord. Chem. Rev.*, **203**, 151 (2000); (c) K. Umakoshi, Y. Yamauchi, K. Nakamiya, T. Kojima, M. Yamasaki, H. Kawano, M. Onishi. *Inorg. Chem.*, **42**, 3907 (2003).

[18] (a) J.E. Cosgriff, G.B. Deacon. *Angew. Chem. Int., Ed. Engl.*, **37**, 286 (1998); (b) G.B. Deacon, E.E. Delbridge, B.W. Skelton, A.H. White. *Angew. Chem. Int., Ed. Engl.*, **37**, 2251 (1998); (c) G.B. Deacon, C.M. Forsyth, A. Gitlits, R. Harika, P.C. Junk, B.W. Skelton, A.H. White. *Angew. Chem. Int., Ed. Engl.*, **41**, 3249 (2002); (d) I.A. Guzei, A.G. Baboul, G.P.A. Yap, A.L. Rheingold, H.B. Schlegel, C.H. Winter. *J. Am. Chem. Soc.*, **119**, 3387 (1997); (e) D. Pfeiffer, M.J. Heeg, C.H. Winter. *Inorg. Chem.*, **39**, 2377 (2000).

[19] J.R. Perera, M.J. Heeg, H.B. Schlegel, C.H. Winter. *J. Am. Chem. Soc.*, **121**, 4536 (1999).

[20] (a) A. Cingolani, S. Galli, N. Masciocchi, L. Pandol, C. Pettinari, A. Sironi. *Dalton Trans.*, 2479 (2006); (b) R. Sarma, D. Kalita, J.B. Baruah. *Dalton Trans.*, 7428 (2009); (c) U.P. Singh, P. Tyagi, S. Pal. *Inorg. Chim. Acta*, **362**, 4403 (2009); (d) J. Li, Y.H. Xing, H.Y. Zhao, Z.P. Li, C. Guang Wang, X.Q. Zeng, M.F. Ge, S.Y. Niu. *Inorg. Chim. Acta*, **362**, 2788 (2009).

[21] J. Li, J.H. Zhou, Y.Z. Li, L.H. Weng, X.T. Chen, Z. Yu, Z. Xue. *Inorg. Chem. Commun.*, **7**, 538 (2004).

[22] S.W. Jin, D.Q. Wang, W.Z. Chen. *Inorg. Chem. Commun.*, **10**, 685 (2007).

[23] S.W. Jin, W.Z. Chen. *Inorg. Chim. Acta*, **360**, 3756 (2007).

[24] S.W. Jin, W.Z. Chen. *Polyhedron*, **26**, 3074 (2007).

[25] Bruker. *SMART* and *SAINT*. Bruker AXS Inc., Madison, WI, USA (2004).

[26] *SHELXTL-PC (Version 5.03)*, Siemens Analytical Instruments, Madison, WI (1994).

[27] M. Padmanabhan, S.M. Kumary, X.Y. Huang, J. Li. *Inorg. Chim. Acta*, **358**, 3537 (2005).

[28] Y.J. Sun, P. Chen, S.P. Yan, D.Z. Liao, Z.H. Jiang, P.W. Shen. *J. Coord. Chem.*, **55**, 363 (2002).

[29] X.M. Chen, Z.T. Xu, X.C. Huang. *J. Chem. Soc., Dalton Trans.*, 2331 (1994).

[30] B. Singh, J.R. Long, F. De Biani, D. Gatteschi, P. Stavropoulos. *J. Am. Chem. Soc.*, **119**, 7030 (1997).

[31] J. Bernstein, R.E. Davis, L. Shimoni, N.L. Chang. *Angew. Chem. Int. Ed.*, **34**, 1555 (1995).

[32] Z.D. Tomic, Z.K. Jacimovic, V.M. Leovac, V.I. Cesljevi. *Acta Crystallogr., Sect. C*, **56**, 777 (2000).

[33] H.L. Chun, D.N. Dybtsev, H. Kin, K. Kim. *Chem. Eur. J.*, **11**, 3521 (2005) and references therein.